Air Flow Characteristics inside an Industrial Wood Pallet Drying Kiln

Adrian-Gabriel Ghiaus [*,1], Marian-Andrei Istrate[1] and Andrei-Mugur Georgescu[1]
[1]Technical University of Civil Egineering, Bucharest
*Corresponding author: bd. Pache Protopopescu nr.66, Bucuresti Sector 2, ROMANIA,
ghiaus@instalatii.utcb.ro

Abstract: Analysis and optimization of air flow distribution inside drying kiln systems contribute to the improvement of the final product quality. The present study reports on the three-dimensional numerical solution of air flow within a drying kiln enclosure. The air flow field is examined in different configurations and operation conditions. Depending on the off/on switched fans, we obtain various air flow distributions. The simulation was performed using the Comsol Multiphysics program using the k-ε turbulent mode in steady-state regime. The effect of the turbulence modeling is distinguished through a direct comparison between the results. The results highlight the position of the recirculation regions and the distribution of the air flow.

Keywords: drying, air flow, simulation

1. Introduction

Due to the rapid growth of the industrial utilization and of the need to obtain dry wooden components, natural drying, which takes at least 2-5 years, has become inappropriate for the current demands. Therefore, searching for wood drying acceleration methods that do not affect the wood structure has become a necessity nowadays. Convective drying is one of the most used processes and the quality of the final dried product depends on the uniformity of the drying air distribution. The analysis of the velocity field was carried out by simulation using the Comsol Multiphysics numerical modeling software. First of all, there were chosen the steady-state conditions for the flow regime and the three-dimensional space for the computational domain.

Four different operation solutions were analyzed:

- a) two recirculation fans situated on opposite sides and at different heights are running;
- b) four recirculation fans situated in pairs of two on opposite sides are running;
- c) four recirculation fans and one exhaust fan are running and there is an open air slit;
- d) one exhaust fan is running and there is an open air slit.

From the above described cases, the first two are presented in this paper.

The simulation results are presented as 3D velocity distribution diagrams corresponding to certain zones inside the kiln. The analysis of the results leads to the adjustment of the operation parameters and to the space optimization of the fan arrangement, in order to obtain the maximum efficiency.

2. Computational modeling

2.1. Geometry of the drying kiln

The 3D view of the considered industrial type of wood drying kiln is shown in Figure 1. The drying unit system consists of a kiln chamber inside which there are four recirculation fans and on this chamber there is an exhaust fan.

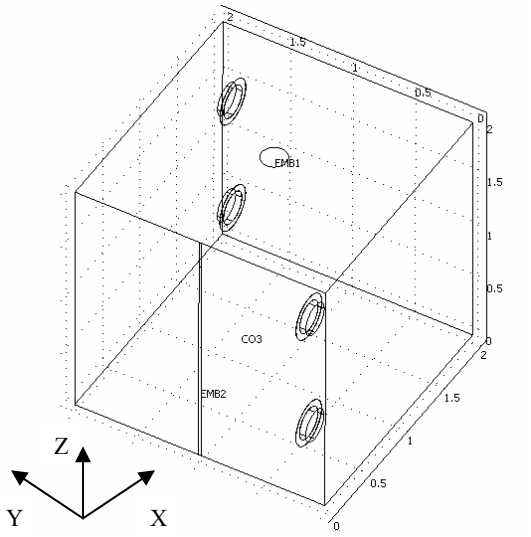

Figure 1. The 3D view of the wood drying kiln.

Because the exhaust fan doesn't work correctly without fresh air, it is necessary to mount a fresh air slit on the vertical front side. The kiln chamber is considered a cube with a two-meter long edge. The diameter of the recirculation fans is 250mm and of the exhaust fan is 200mm. The fresh air slit has a height of 2000mm and a width of 40mm. These fans are situated at different heights and on opposite sides.

2.2. Boundary conditions and mesh cells

The boundary conditions for the air flow are determined by the performance of the axial flow fan. The total air volume flow rate through the kiln chamber is given by the pressure jump across the axial fan and its value results from the performance curves of the fan. At the inlet, uniform velocity distribution is assumed (v_0=0.7m/s) and this corresponds to Q_0=123.7m³/h. The turbulence models are valid only in fully turbulent regions. Close to the wall, where viscous effects become dominant, the models are used in conjunction with the wall functions. For this study, the convectional equilibrium logarithmic law governing the wall is used. The computational domain is meshed and fine grid spacing close to all the walls has been applied, in order to resolve steep gradients. The grids for the drying kiln consist of 150.000 elements and the result of this can be seen in Figure 2.

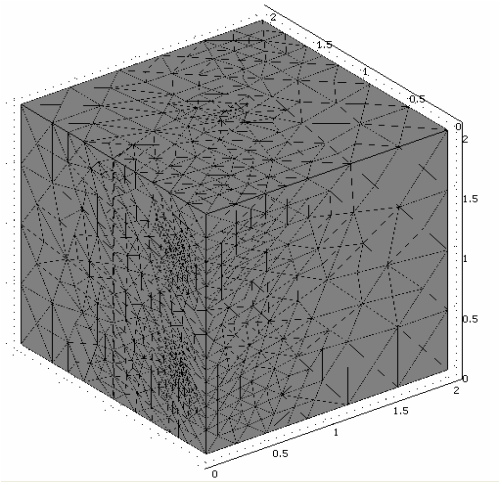

Figure 2. The 3D view of the meshed wood drying kiln.

2.3. Numerical simulation of the inside fans

In order to accurately model the inside fans without having to model the geometry of the blades and rotate them throughout the simulation a hybrid approach was used, i.e. the action of the blades on the air was introduced as volume forces in the Navier-Stokes equations for the sub-domains representing the fans. First, the fans were modeled as different cylindrical sub-domains in the kiln. Fluid characteristics of the sub-domains (temperature, density and viscosity) were considered the same as the ones in the kiln i.e. t = 20 °C, ρ = 1.21 kg/m³ and $\eta = 1.98 \cdot 10^{-5}$ Pa·s. Only the volume forces terms on the three axes were different. Second, the pressure drop vs. flow rate curve of the fans was approximated by a 3rd order polynomial to yield a function $\Delta p(Q)$. Third, an integration coupling variable was set on the boundary representing the inlet cross-section of each interior fan. In this variable the program integrates the velocity component normal to the inlet cross-section (i.e. axial inlet velocity in the fan) which gives the flow-rate trough the fan at each iteration Q. Finally, we introduced in each sub-domain, in the volume force corresponding to the axial direction for each inside fan, the formula of the pressure-drop computed with the corresponding variable representing the flow-rate, divided by the length of the fan (in order to get, in each cell of the sub-domain a volume force that would yield in the outlet section of the fan the pressure drop corresponding to the flow rate for each iteration). Axial fans also induce a rotational velocity component at the outlet. In order to introduce this component as volume forces in the sub-domains, we have to analyze the velocity triangles for axial hydraulic machineries (Figure 3), where inlet velocities are colored in blue and denoted with subscript 1, while outlet velocities are colored in red and denoted with subscript 2.

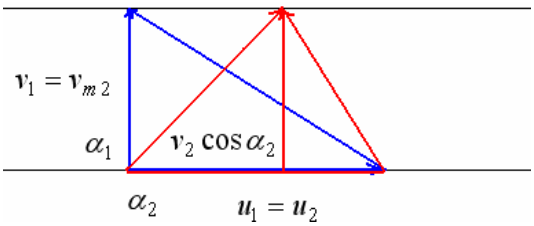

Figure 3. Velocity triangles for axial hydraulic machineries

As the inlet velocity is considered normal to the fan inlet cross-section, and the flow rate trough the fan is constant this results in an equal meridian velocity at the outlet v_{m2}. On the other hand the transport velocity is known as long as we know the rotating speed of the fan (n) and the radius where we perform the computation (r):

$$u_1 = u_2 = 2\pi n r$$

The fundamental equation for turbo machineries is:

$$H_{T\infty} = \frac{1}{g}(u_2 v_2 \cos\alpha_2 - u_1 v_1 \cos\alpha_1)$$

which, for an axial fan with normal inlet velocity ($\alpha_1 = 90^o$), yields:

$$\Delta p = \rho u_2 v_2 \cos\alpha_2$$

Hence the tangential component of the velocity is:

$$v_2 \cos\alpha_2 = \frac{\rho g H_{T\infty}}{\rho \eta_h u_2} = \frac{\Delta p}{\rho 2\pi n r}$$

This component is only a function of constant rotating speed of the fan, pressure drop and radius with respect to the centre of the fan where calculations are made. It can also be included as volume forces in the sub-domain representing the fans if geometrically decomposed with respect to the two axes that are normal to the axis of the fan. This is a simple geometrical transformation as long as we know the coordinates of the cell in which the term is added. A problem is still the presence of the radius in the denominator of the equation. This means that cells situated near the axis of the fan $r \cong 0$ will yield infinity when computing the tangential component of the velocity.

The model of the fan can not be a simple cylinder but rather an annular shape in order to bypass this problem. In fact the annular shape model is closer to an real axial fan than the cylindrical model as any axial fan has a shaft that does not permit air flow trough the exact centre of the fan.

Several simulations were performed both with the complete model (i.e. both axial and tangential volume force terms) and with the simplified model (i.e. only axial volume forces terms).By comparing the results and the corresponding computational times we finally adopted the simplified model for the inside fans of the kiln. The tangential component of the volume forces has shown to be very small with respect to the axial one and disappeared almost instantly after the air left the fan. It also increased the computational time by a factor of 2 with respect to the simplified model. In the sequel this simplified model was used for all simulations.

The simulation was performed based on the Navier Stokes equation:

$$\rho\left(\frac{\partial V}{\partial t} + V\,\nabla V\right) = -\nabla p + \mu\,\nabla^2 V + F$$

where $\rho\left(\frac{\partial V}{\partial t} + V\,\nabla V\right)$ is the vector tensor form, ∇p is the pressure, μ is the viscosity and F is the specified force.

3. Results and discussion

In the first analyzed case, two fans placed at different heights and on opposite sides are running. First of all, two sections along the central axis, on the running direction of the fans were taken into consideration. We can observe the velocity distribution on the analyzed plane as a red colored surface. We can see in Figure 4 a 3D representation of the plane.

In Figure 5, the velocity distribution is represented in a vectorial form, using a 3D coordinate system. We can notice the air flow inside the kiln, the intensity of the air flow when exiting the fan and also the decrease of the intensity when the air spreads into the chamber.

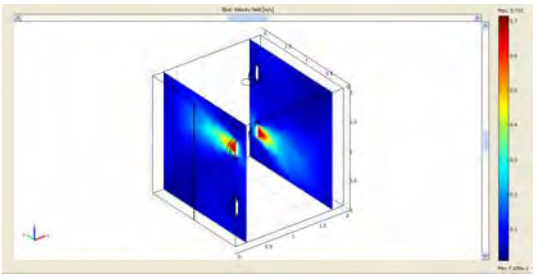

Figure 4. Velocity distribution

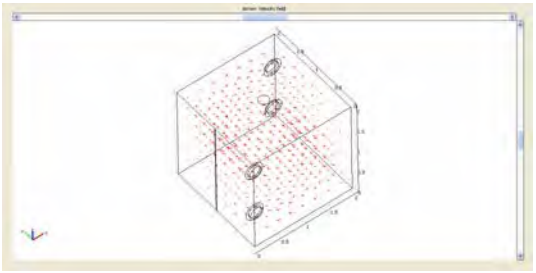

Figure 5. Velocity distribution in a vectorial form

In the middle of the drying kiln there are some recirculation areas where the velocities have much smaller values than those obtained at the output of the fan. We observe that the corners of the kiln are the least exposed to the air flow.

Figure 6 illustrates a vectorial representation as well as a graphical representation (the colored one) of the air flow in a 3D image.

In Figure 7 there is a section belonging to the Y-Z plane, placed in the centre of the fan and along the air flow direction where the intensity is maximum.

Figure 8 depicts the intensity of the velocity field as it appears from the X-Z plane. We can observe the most exposed areas of each fan.

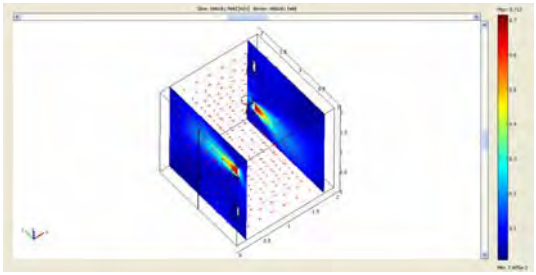

Figure 6. Vector and contour of velocity distribution

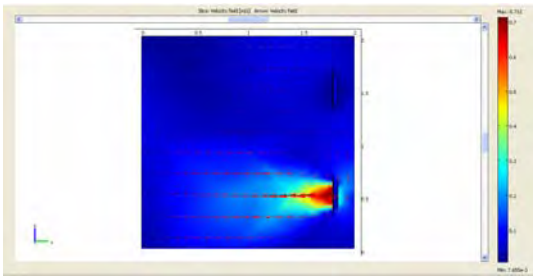

Figure 7. Y-Z plane section of velocity distribution

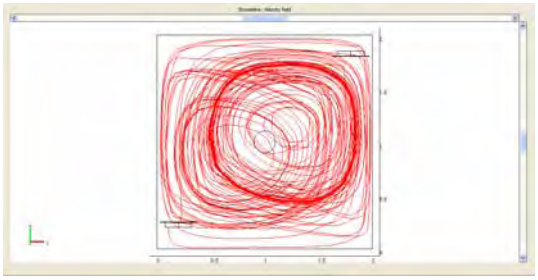

Figure 8. X-Z plane section of path lines

In the second analyzed case all the four fans positioned in groups of two at the same height but having different orientations are running. In Figure 9 we can observe, as in the previous case (when only two of the fans were running), two vertical sections cut along the central axis of the fan (Y-Z plane). The velocity distribution is represented as a colored surface in a 3D view.

A more explicit image appears in Figure 10 which illustrates a 2D vertical section along Y-Z.

In Figure 11 there is a vectorial form of the velocity distribution in a three dimensional coordinate system. We can see the air flow direction and also the velocities in certain places of the kiln.

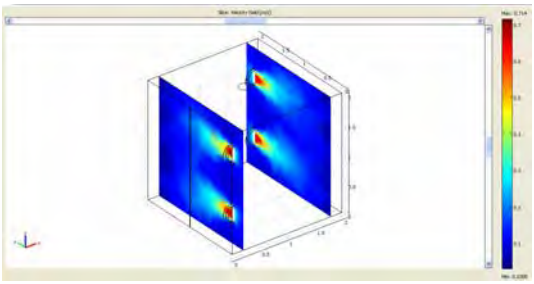

Figure 9. Vector and contour of velocity distribution

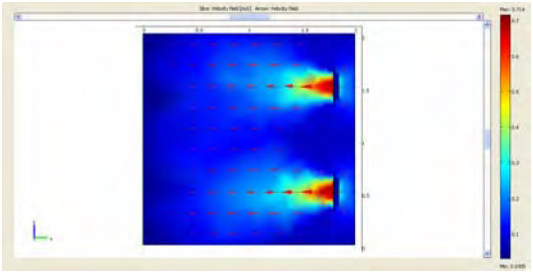

Figure 10. Y-Z plane section of velocity distribution

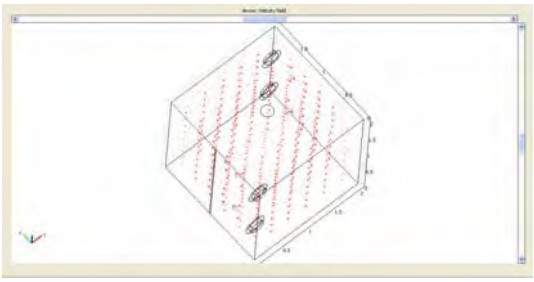

Figure 11. Velocity distribution in a vectorial form

4. Conclusions

In contrast with the first case, in the second case the air flow circulation inside the kiln has a higher intensity and a uniform distribution. Another observation that can be stated is related to the existence and position of recirculation zones near the kiln corners. Similar results were obtained with the other configuration including beside the recirculation fans an exhaust fan situated on the kiln roof and a fresh air slit. Further investigations are foreseen by simulation the positions of the four recirculation fans, placing them at different coordinates or by changing the number of fans having different positions and heights. Moreover, it could be simulated more complex kiln geometries and the result analysis and interpretation together with the previous conclusions will indicate the best solutions for design purpose.

5. References

1. Sun Z.F., Carrington C.G., Anderson J.A. & Sun Q., Air flow patterns in dehumidifier wood drying kilns, *IChemE, Chemical Engineering Research and Design*, **Volume 82**, page numbers 1344-1352 (2004)

2. *New Food Engineering Trends*, p.p. 45-102, Nova Science Publishers, Inc., New York (2008)

3. Margaris D.P. & Ghiaus A.-G., Dried products quality improvement by air flow manipulation in tray dryers, *Journal of Food Engineering*, **Volume 75**, page numbers 542-550 (2006)

4. Tabsoba M., Moureh J. & Flick D., Airflow patterns in an enclosure loaded with slotted pallets, *International Journal of Refrigeration*, **Volume 29**, page numbers 899-910 (2006)

5. Mathioulakis E., Karathanos V. T. and Belessiotis V. G., Simulation of air movement in a dryer by computational fluid dynamics: Application for the drying if fruits, *Journal of Food Engineering*, **Volume 36**, page numbers 183-200 (1998)

6. Sun Z.F., Carrington C.G., Anderson J.A. and Sun Q., Air flow patterns in dehumidifier wood drying kilns, *Chemical Engineering Research and Design*, **Volume 82**, page numbers 1344-1352 (2004)

6. Acknowledgements

This research was carried out in the framework of "MicroDry" project partly funded by Romanian "Innovation" program - PNCDI-II.